Reaction Chemistry & Engineering

COMMUNICATION

View Article Online
View Journal | View Issue

Cite this: *React. Chem. Eng.*, 2019, 4, 273

Received 1st October 2018,
Accepted 4th December 2018

DOI: 10.1039/c8re00233a

rsc.li/reaction-engineering

Effect of metal chlorides on glucose mutarotation and possible implications on humin formation†

Pranav Ramesh, Athanasios Kritikos and George Tsilomelekis *

An *in situ* Raman spectroscopic kinetic study of the glucose mutarotation reaction is presented herein. The effect of metal chlorides on the ease of the ring opening process is discussed. It is shown that $SnCl_4$ facilitates the mutarotation process towards the β-anomer extremely fast, while $CrCl_3$ appears to promote the formation of the α-anomer of glucose. The infrared spectra of humins prepared in different Lewis acids underscore the possibility of multiple reaction pathways.

Introduction

Converting biomass, a renewable source of carbon, to value-added products is a promising and sustainable approach for biofuel/biochemical production with immense benefits to several industrial sectors. Carbohydrates, aldoses and/or ketoses, derived from cellulosic/hemicellulosic constituents of non-edible biomass sources, are excellent candidates for chemical production but the high oxygen content in their structure requires further downstream processes.[1,2] The pivotal impact of the selective conversion of these monosaccharides to their dehydration counterparts as intermediates has been underscored in recent years.[3,4] A characteristic example encompasses the conversion of cellulose-derived glucose to 5-hydroxymethylfurfural (5-HMF) which is considered as one of the key biomass-derived intermediates.

Glucose isomerization to fructose is an important intermediate reaction in the production of 5-hydroxymethylfurfural from cellulosic biomass sources and it is well established that it is Lewis acid-catalyzed. The presence of Lewis acids is believed to facilitate glucose ring-opening in aqueous solution, followed by a kinetic relevant intramolecular hydride shift from C_2 to the C_1 position of glucose.[5] The ease of the first step, *i.e.* ring opening, in the presence of metal chlorides in ionic liquids has been reported by means of DFT calculations.[6] It has also been suggested that the possible changes in the anomeric equilibrium, especially *via* the stabilization of the α-anomer of glucose, might be responsible for the improved selectivity towards fructose.[7,8] This also agrees with the concept of anomeric specificity of enzymes; for instance, immobilized D-glucose isomerase has shown ~40% and ~110% higher conversion rates starting from α-D-glucose as compared to equilibrated glucose and β-D-glucose solutions, respectively.[9] Production of 5-HMF in ~60% yield has been reported by coupling homogeneous Lewis with Brønsted acids in a tandem glucose isomerization and fructose dehydration scheme (Scheme S1†).[10]

Herein, we report an *in situ* Raman kinetic study on the ease of glucose mutarotation in the presence of $AlCl_3$, $CrCl_3$ and $SnCl_4$ homogeneous Lewis acid catalysts. The rationale behind choosing these metal salts lies in the fact that although all three salts have proven to facilitate glucose isomerization under various reaction conditions the product

Department of Chemical and Biochemical Engineering, Rutgers, The State University of New Jersey, Piscataway, 08854, NJ, USA. E-mail: g.tsilo@rutgers.edu

† Electronic supplementary information (ESI) available. See DOI: 10.1039/c8re00233a

George Tsilomelekis

George Tsilomelekis is an Assistant Professor in the Department of Chemical and Biochemical Engineering at Rutgers University. His research interests lie at the intersection of material synthesis, catalysis and reaction engineering with endeavors to be placed on establishing structure–reactivity relationships via the rational implementation of molecular spectroscopic techniques under real reaction conditions (operando spectroscopy). His specific research directions encompass the unravelling of solvent effects in biomass processing as well as understanding of active sites in alkane dehydrogenation reactions. Dr. Tsilomelekis is the recipient of the National Science Foundation CAREER award as well as the American Chemical Society Doctoral New Investigator award.

distribution varies significantly, with $AlCl_3$ and $CrCl_3$ being more selective. $SnCl_4$ has reported to facilitate the glucose isomerization reaction in the temperature range of 130–150 °C; however, the process suffers from significant formation of side reactions (humins), thus sacrificing the product selectivity. We believe that metal chlorides, as Lewis acids, can potentially affect the product selectivity in biomass reactions by altering a) the kinetics of ring opening and b) the equilibrium level of the mutarotation process as well as by c) introducing additional pathways towards degradation reactions.

Results and discussion

Glucose mutarotation and Raman spectral considerations

For the quantitative estimation of the anomeric species distribution of glucose in aqueous solutions, many methods have been reported in the open literature. Besides the well-established polarimetric method, molecular spectroscopic techniques have proven to provide comparable and accurate results.[11] Vibrational spectroscopy techniques, Raman and FTIR, have been routinely used to study also solid-state glucose mutarotation reactions, solvent and cation effects on the anomeric equilibrium, *etc. In situ* Raman detection of solid state glucose mutarotation has been also reported, but spectral deconvolution using Gaussian peaks is required, thus making the analysis time consuming. For Raman spectroscopy, the well-accepted method proposed by Mathlouthi *et al.* involves the ratio of the C_2–C_1–O_1 bending mode of the α- and β-anomers, *i.e.* $I_{543}/(I_{543} + I_{520})$, for the calculation of the anomeric equilibrium.[12] Although this ratio well estimates the anomeric equilibrium, spectral overlapping limits the accuracy of this method in the whole kinetic profile. This limitation can be overcome by rationalizing the vibrational assignments of the pure aqueous glucose anomers *via* the study of their kinetic profiles, as discussed next.

In Fig. 1a, we show for comparison the Raman spectrum of the crystalline glucose used. The 541 cm^{-1} band is characteristic of the contribution of the C_2–C_1–O_1 bending mode of the α-anomer of glucose. The corresponding C_2–C_1–O_1 bending mode of the β-anomer is expected to appear at 518 cm^{-1}, which is absent in our crystalline sample, confirming the purity of the sample used. Upon dissolution in water, Fig. 1b, characteristic bands of α-glucose (t = 0 min) become broader and shift slightly to higher frequencies. A noticeable change encompasses the appearance of a new band at 515 cm^{-1} that almost coexists in frequency with the suggested C_2–C_1–O_1 bending mode of the β-anomer (518 cm^{-1}). Since the spectrum is taken after complete glucose dissolution (t = 0 min indicates the time of collection of the first spectrum and not the time of mixing) one expects small progress in glucose mutarotation to result in the formation of β-anomers that can overlap in the Raman spectrum. However, we support that the 515 cm^{-1} peak is characteristic of the α-anomer of glucose since the Raman kinetic data reported in Fig. 1c shows a slight decrease of the intensity of the 515 cm^{-1} and the appearance of a neighboring band at 519 cm^{-1} with time. The previous argument is also supported by the clear isosbestic points which appear around the 515 cm^{-1} band confirming clear transition of α- to β-anomers with time.

The spectral envelop within the 200–600 cm^{-1} range is sensitive to the conformational changes of aqueous monosaccharides (and polysaccharides) since usually more than one vibrational motion contributes to each observed peak.[13] Theoretical calculations of the vibrational modes of glucose as well as experimental Raman/IR and Raman optical activity measurements have shown that skeletal endocyclic and exocyclic modes might coexist with bands that usually are dealt as "purely" anomeric modes. Corbett *et al.*[14] studied the vibrational modes of "wet" α-D-glucose and suggested that the 538 cm^{-1} band is conformation-sensitive and upon interaction with water shifts to 512 cm^{-1} and 522 cm^{-1}. This is further supported by the work of Mathlouthi *et al.* where modes involving vibration of the CH_2 group show shifts in frequencies more than ~10 cm^{-1} upon changing the D-glucose (or sucrose) concentration.[15] Deconvolution of the

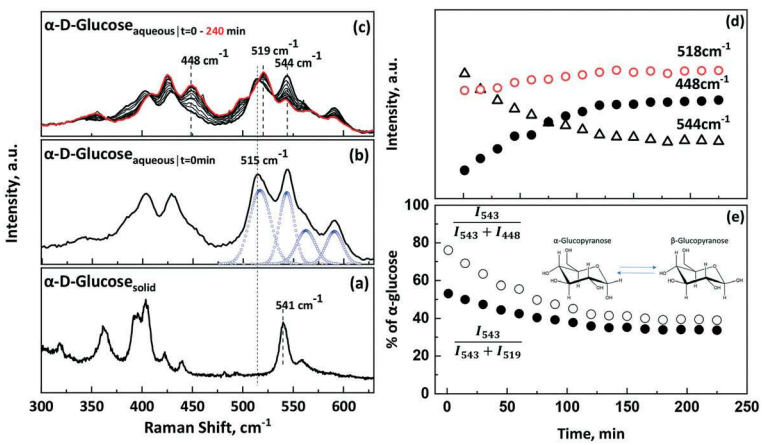

Fig. 1 Raman spectra of α-glucose in a) solid, b) water and c) under mutarotation reaction. Analysis of the spectra is shown in d) and e).

500–600 cm^{-1} range in our spectra shows four peaks located at 515, 544, 564 and 590 cm^{-1}, which is in very good agreement with those reported in the literature. Theoretical studies *via* first principle calculations can shed more light on how the interactions of glucose with water molecules can affect the vibrational modes observed.

In Fig. 1c we show the *in situ* Raman of the aqueous α-D-glucose solution as it undergoes mutarotation in the 300–650 cm^{-1} range. Since all the spectra presented herein correspond to glucose in aqueous solutions, the spectral contribution from water as well as the quartz cuvette used has been subtracted. In addition, prior to the subtraction, all the spectra have been normalized with respect to the total area of each spectrum. As the mutarotation reaction progresses, new Raman bands at 425, 448 and 519 cm^{-1} evolve at the expense of the bands that correspond to the α-anomer of glucose. The band located at 448 cm^{-1} (C–C–O skeletal mode as well[13,15]) has almost no spectral overlap from the neighbouring bands, and thus we have used this peak as the characteristic peak of the β-anomer instead of the 520 cm^{-1} band. As can be seen in Fig. 1d, the relative intensities of the 518 and 544 cm^{-1} bands at early reaction times are almost identical indicating that the ratio $I_{543}/(I_{543} + I_{520})$ underpredicts the % change of the α-anomer at the beginning. This limits significantly our ability to accurately measure the anomeric concentrations that could potentially help us to understand the catalytic behavior in downstream reactions, such as isomerization, dehydration, *etc.* This is also shown in Fig. 1e (solid circles). After 200 min of reaction, this ratio predicts ~34% α- and ~66% β-anomers, which is in agreement with the expected equilibrium level.[16] Research on the solid state mutarotation of crystalline and amorphous glucose by means of *in situ* Raman spectroscopy has shown that the $I_{543}/(I_{543} + I_{520})$ ratio captures the kinetic profiles in the whole range.[17] This is achieved probably due to the fact that in the solid state, α-glucose does not present the same conformational flexibility, possible hydrogen bonding or multiple configurations, and thus no overlap in the characteristic 520 cm^{-1} band of the β-anomer appears. Herein, we show that by utilizing the 448 cm^{-1} peak as the characteristic peak of the β-anomer of glucose, which clearly appears with the same rate the corresponding α-anomer disappears, we predict accurately both the early and late stages of the mutarotation reaction in the liquid phase which is in excellent agreement with literature reports on kinetic data in water. Thus, all the Raman spectra shown here have been analyzed with respect to the $I_{543}/(I_{543} + I_{448})$ ratio.

Effect of metal chlorides on glucose mutarotation

In Fig. 2, we present the Raman spectra of aqueous glucose solutions under the mutarotation reaction in the presence of 50 mM $AlCl_3$, $CrCl_3$ and $SnCl_4$. The *in situ* Raman spectra under different catalyst concentrations are not shown here for brevity (see the ESI†). Upon addition of metal chlorides in glucose aqueous solution, we observe a clear change in the

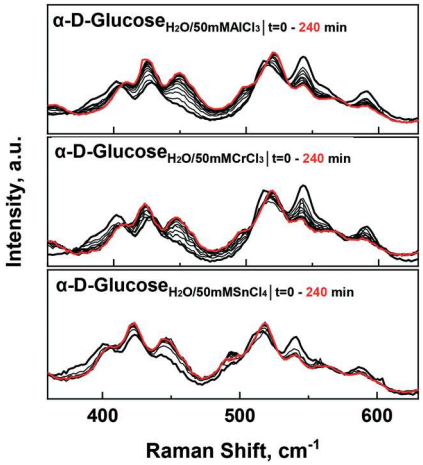

Fig. 2 *In situ* Raman spectra of glucose mutarotation reaction.

kinetics of mutarotation between $AlCl_3$, $CrCl_3$ and $SnCl_4$. Particularly, $SnCl_4$ facilitates glucose mutarotation much faster than the other metal salts under the same concentration. The kinetics of glucose mutarotation become even faster at concentrations that reach 100 mM for both catalysts, with $SnCl_4$ exhibiting always the highest rates based on the relative disappearance of relevant bands for α- and β-anomers. In the case of 100 mM $CrCl_3$, the observed kinetics of mutarotation is fast as well (see rate constants in the ESI†). By utilizing the $I_{543}/(I_{543} + I_{448})$ ratio as described earlier, in Fig. 3(a–c), we present the kinetic profiles of glucose mutarotation as described by the change in the α-anomer, in the range of 10–100 mM catalyst concentration and compare them with the rates in neat water. Conducting the glucose mutarotation reaction in 10–50 mM $AlCl_3$ we observe similar rates to neat water, while increasing the concentration to 100 mM, we reach equilibrium approximately 50 min faster. Our observation regarding the effect of $AlCl_3$ on mutarotation rates is in agreement with those reported by Hu and co-workers,[18] where enhanced mutarotation rates (at room temperature) were observed *via* ATR-FTIR spectroscopy. In this work, it was suggested that the presence of $[Al(OH)_{2(aq)}]^+$ species promotes both glucose ring opening/closing reactions (mutarotation) and glucose isomerization to fructose. The same group recently confirmed their previous argument regarding the existence of $[Al(OH)_{2(aq)}]^+$ species under these reaction conditions by using electrospray ionization-mass spectroscopy (ESI-MS) coupled with infrared spectroscopy.[19] Vlachos and co-workers have shown by coupling pH measurements, speciation model prediction with qNMR and dynamic light scattering techniques that the same partially hydrolyzed aluminum species is also the active species for glucose isomerization to fructose.[20] In contrast, the concentration of $SnCl_4$ appears to have a monotonic effect on glucose mutarotation rates, *i.e.* the higher the concentration of $SnCl_4$, the higher the rate of mutarotation. We believe that the enhanced rates observed are due to the competitive effect of Brønsted and Lewis

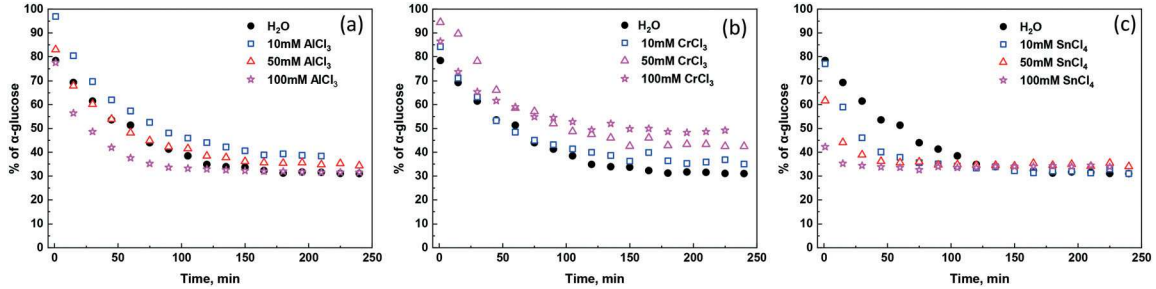

Fig. 3 Kinetics profiles from *in situ* Raman spectroscopic data for (a) $AlCl_3$, (b) $CrCl_3$ and (c) $SnCl_4$. Kinetic data in water shown also for comparison. Analysis has been performed by utilizing the $I_{543}/(I_{543} + I_{448})$ ratio of skeletal modes of glucose.

acidity. Upon dissociation of metal chlorides in water into Me^{z+} and Cl^-, the $[M(OH_2)_n]^{z+}$ species will undergo hydrolysis and protons will be released as follows:

$$[M(OH_2)_n]^{z+} + xH_2O \leftrightarrow [M(OH)_x(OH_2)_{n-x}]^{(z-x)+} + xH_3O^+$$

Specifically, when $SnCl_4$ is dissolved in water, the hexaaqua $[Sn(OH)_x(H_2O)_{6-x}]^{(4-x)+}$ complex dominates the solution at concentrations below 100 mM (concentration range of this study).[21] Mesmer *et al.* have shown that the hydrolysis of aluminum ions is kinetically slow at temperatures pertinent to our work, indicating that the pH of $AlCl_3$ solutions will be fairly stable throughout the reaction. The pH values of the solutions at different stages of the experiments are listed in Table S2.† We clearly see that for the case of $SnCl_4$, the rate of glucose mutarotation correlates very well with the pH values; the lower the pH, the faster the rate. This is in agreement with the proposed general acid catalyzed mechanism for this reaction. We also support this argument by conducting the mutarotation in the presence of Brønsted acids and analyzing their relevant kinetics (Fig. S3†). However, considering solutions with similar pH ~2.9 (50 mM $CrCl_3$ and 100 mM $AlCl_3$), we observe that in $AlCl_3$, the observed rate values as reported in Table S1† are much higher than in $CrCl_3$ underscoring that the nature of the salt used plays an important role in the mutarotation reaction in the low Brønsted acidity regime. Since the reaction mechanism might occur *via* a stepwise or concerted mechanism where two proton transfers are involved,[22,23] the nature of salt species in the local environment around glucose can potentially affect the transition state thus affecting the observed rates. However, further mechanistic work involving first principle calculations and molecular dynamics studies as well as more advanced spectroscopic techniques is needed in order to disentangle the effect of the aqueous species in facilitating ring opening and closing of glucose as compared to Brønsted acids.

It is noteworthy here that we did not observe any significant change in the equilibrium of α- and β-glucose anomers for $AlCl_3$ and $SnCl_4$. In all cases, ~35–40% α- anomer and 60–65% β-anomer were present at equilibrium. However, a monotonic increase in the percentage of the α-anomer was observed upon increasing the concentration of $CrCl_3$. Interestingly, at 100 mM $CrCl_3$, the percentage of the α-anomer increased to almost 50% as opposed to ~34% in neat water. In the pioneering work by Zhang and co-workers, it was inferred that $CrCl_3$ might stabilize the α-anomer thus accelerating isomerization rates.[7] However, since the present data pertain to room temperature, no direct conclusions can be drawn quickly with respect to temperatures pertinent to the isomerization reaction. In order to bridge the temperature gap in the proposed approach, future research work pertaining to the rational design of high-temperature optical liquid phase reactors in conjunction with mathematical handling of highly overlapping spectra (*e.g.* principal component analysis and/or 2D correlation Raman spectroscopy) is considered an essential element. Although our Raman data provide useful qualitative as well as quantitative information regarding the changes occurring in the mutarotation reaction of glucose in the presence of metal chlorides, utilizing other spectroscopic techniques, such as NMR, can provide more insights into the actual anomeric distribution (pyranoses *vs.* furanoses and open chain) in equilibrium as well as interactions between glucose and active species at higher temperatures.

Effect of metal chlorides on the humin molecular structure

There are many experimental and theoretical pieces of evidence in the open literature suggesting that the interaction of aqueous metal species with sugars and/or furanic compounds can lead to enhanced rates towards by-products, such as humins. Understanding by-product formation in biomass conversion is an essential component either in process optimization or in by-product valorization. We have performed sugar degradation reactions (either with glucose or fructose) to intentionally produce humins for further study. The reaction time was 24–48 h to ensure high conversion of sugars at 120 °C. The ATR-FTIR spectra of humins (Fig. 4) reveal significant differences in the wavenumber range of 1300–1900 cm^{-1}. We report that humins that are formed in glucose and fructose in the presence of $AlCl_3$ appear to have similar molecular structures. However, in the presence of $SnCl_4$, we observe changes in the relative absorbance of the peaks located at ~1600 and ~1700 cm^{-1} which are ascribed to C=C and C=O stretching modes.[24–26] This observation indicates

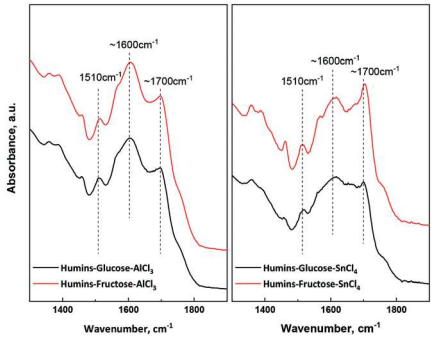

Fig. 4 ATR-FTIR spectra of humins formed in $AlCl_3$ and $SnCl_4$ solutions.

that in humins prepared in $AlCl_3$, substituted furans are present as underscored by the 1600 cm^{-1} band that could arise *via* the HMF route. However, in $SnCl_4$ the 1700 cm^{-1} band indicates the presence of C=O modes probably due to incorporation of carboxylic acids, aldehydes and ketones.[24] We hypothesize that the ease of ring opening of glucose in conjunction with the intrinsic acidity of $SnCl_4$ solutions leads possibly to the formation of these intermediates which in turn promote the formation of humins at early stages of reaction without passing the "HMF to DHH route". This argument is further supported by the small spectral contribution of furan rings (~1520 cm^{-1}) in $SnCl_4$ as opposed to $AlCl_3$-derived glucose humins. When fructose is used as a reactant, both $AlCl_3$ and $SnCl_4$ show the characteristic C=C stretching of furanic rings indicating that the HMF degrades to humins.

Conclusions

We have used *in situ* Raman spectroscopy in the liquid phase to monitor the glucose mutarotation reaction. We find that the rates follow the order $AlCl_3 < CrCl_3 < SnCl_4$. Interestingly, we find that the presence of $CrCl_3$ promotes the formation of the α-glucose anomer probably due to the strong interaction of glucose and the dissolved metal species. We also show that the molecular structures of humins formed in the presence of $AlCl_3$ and $SnCl_4$ are quite different; $AlCl_3$ species promote the pathway that involves incorporation of furan rings (possibly HMF to DHH), while $SnCl_4$ species promote probably the fragmentation of glucose and fructose prior to the formation of HMF.

Conflicts of interest

There are no conflicts to declare.

Acknowledgements

This material is based upon work supported in part by Rutgers, The State University of New Jersey and the National Science Foundation Award #1705825.

Notes and references

1 I. Delidovich and R. Palkovits, *ChemSusChem*, 2016, **9**, 547–561.
2 H. Li, S. Yang, S. Saravanamurugan and A. Riisager, *ACS Catal.*, 2017, **7**, 3010–3029.
3 J. N. Chheda, G. W. Huber and J. A. Dumesic, *Angew. Chem., Int. Ed.*, 2007, **46**, 7164–7183.
4 Y. Román-Leshkov, C. J. Barrett, Z. Y. Liu and J. A. Dumesic, *Nature*, 2007, **447**, 982.
5 Y. Roman-Leshkov, M. Moliner, J. A. Labinger and M. E. Davis, *Angew. Chem., Int. Ed.*, 2010, **49**, 8954–8957.
6 E. A. Pidko, V. Degirmenci and E. J. M. Hensen, *ChemCatChem*, 2012, **4**, 1263–1271.
7 H. B. Zhao, J. E. Holladay, H. Brown and Z. C. Zhang, *Science*, 2007, **316**, 1597–1600.
8 B. Wurster and B. Hess, *FEBS Lett.*, 1974, **40**, S105–S111.
9 H. S. Lee and J. Hong, *J. Biotechnol.*, 2000, **84**, 145–153.
10 V. Choudhary, S. H. Mushrif, C. Ho, A. Anderko, V. Nikolakis, N. S. Marinkovic, A. I. Frenkel, S. I. Sandler and D. G. Vlachos, *J. Am. Chem. Soc.*, 2013, **135**, 3997–4006.
11 W. Pigman and H. S. Isbell, *Adv. Carbohydr. Chem.*, 1968, **23**, 11–57.
12 M. Mathlouthi and D. V. Luu, *Carbohydr. Res.*, 1980, **81**, 203–212.
13 E. Wiercigroch, E. Szafraniec, K. Czamara, M. Z. Pacia, K. Majzner, K. Kochan, A. Kaczor, M. Baranska and K. Malek, *Spectrochim. Acta, Part A*, 2017, **185**, 317–335.
14 E. C. Corbett, V. Zichy, J. Goral and C. Passingham, *Spectrochim. Acta, Part A*, 1991, **47**, 1399–1411.
15 M. Mathlouthi, C. Luu, A. M. Meffroybiget and D. V. Luu, *Carbohydr. Res.*, 1980, **81**, 213–223.
16 N. Le Barc'H, J. M. Grossel, P. Looten and M. Mathlouthi, *Food Chem.*, 2001, **74**, 119–124.
17 N. Dujardin, E. Dudognon, J. F. Willart, A. Hedoux, Y. Guinet, L. Paccou and M. Descamps, *J. Phys. Chem. B*, 2011, **115**, 1698–1705.
18 J. Tang, X. Guo, L. Zhu and C. Hu, *ACS Catal.*, 2015, **5**, 5097–5103.
19 J. Tang, L. Zhu, X. Fu, J. Dai, X. Guo and C. Hu, *ACS Catal.*, 2016, **7**, 256–266.
20 A. M. Norton, H. Nguyen, N. L. Xiao and D. G. Vlachos, *RSC Adv.*, 2018, **8**, 17101–17109.
21 K. R. Enslow and A. T. Bell, *Catal. Sci. Technol.*, 2015, **5**, 2839–2847.
22 P. Wlodarczyk, M. Paluch, A. Wlodarczyk and M. Hyra, *Phys. Chem. Chem. Phys.*, 2014, **16**, 4694–4698.
23 N. M. Ballash and E. B. Robertson, *Can. J. Chem.*, 1973, **51**, 556–564.
24 I. van Zandvoort, Y. Wang, C. B. Rasrendra, E. R. H. van Eck, P. C. A. Bruijnincx, H. J. Heeres and B. M. Weckhuysen, *ChemSusChem*, 2013, **6**, 1745–1758.
25 Z. W. Cheng, J. L. Everhart, G. Tsilomelekis, V. Nikolakis, B. Saha and D. G. Vlachos, *Green Chem.*, 2018, **20**, 997–1006.
26 G. Tsilomelekis, M. J. Orella, Z. X. Lin, Z. W. Cheng, W. Q. Zheng, V. Nikolakis and D. G. Vlachos, *Green Chem.*, 2016, **18**, 1983–1993.